Cooperative Soccer Play by Real Small-Size Robot

Kazuhito MURAKAMI[1], Shinya HIBINO[2], Yukiharu KODAMA[2], Tomoyuki IIDA[1], Kyosuke KATO[2], and Tadashi NARUSE[1]

[1] Aichi Prefectural University, Nagakute-cho, Aichi, 480-1198 JAPAN
[2] Graduate School of Information Science and Technology, Aichi Prefectural University, Nagakute-cho, Aichi 480-1198, JAPAN
apurobo@ist.aichi-pu.ac.jp
http://www.aichi-pu.ac.jp/ist/lab/narulab/index.html

Abstract. One of the typical robotic cooperative actions in the RoboCup Small Size [Soccer] League (SSL) is pass play. This paper presents three key technical features necessary for realizing robust pass play between robots. The first of these is a high resolution image processing system which can detect the positions and orientations of the robots concerned. The second one is the control algorithm to move and adjust the robots for the pass play. The third one is the mechanism used to catch a ball moving at high speed. This paper discusses these three things and shows their effectiveness through experimental results.

1 Introduction

The global accademic undertaking known as RoboCup fully supports soccer matches played with robots[1–5]. In order to do so, it is important to achieve robust pass play but there are many key features involved in realizing this type of action. From a software standpoint, it is important to develop and implement a high resolution image processing algorithm able to detect the positions and the orientations of the robots concerned. If an image processing system csnnot detect moving objects correctly or if it takes too much time to do so, it becomes impossible to kick and receive a ball at the location intended. A control algorithm to move and adjust both robots for pass play is also required because without one, a ball will not be passed at the time intended. From a hardware perspective, it is necessary to design a mechanical device capable of catching a ball moving at high speed, because a ball colliding with a given robot at high speed will rebound off of it in an unexpected direction.

Given the preceding considerations, the authors developed a simple but high-speed image processing system with a processing speed about 1.4 msec to detect and track numerous robots and a ball. This was achieved by 1) reducing the searching ranges conducted on images captured by a camera positioned over one SSL field, and 2) implementing an algorithm to control both robots (e.g. the passing and receiving robots) for robust pass play. We improved the each

robot's dribbling mechanism to consistently catch a ball moving at high speed by intentionally adding some leeway in the jointed part of their dribbling device.

In the following sections, the image processing system and cooperative algorithm used to realize pass play are shown in sections 2 and 3, respectively. The mechanical devices for catching a ball and its modeling are shown in section 4.

2 Image Processing System

2.1 Objects to be Detected

According to SSL rules, it is permissible to attach other submarkers to detect the identity number (ID) of each robot and/or their orientation. The number, size and layout of submarkers are unrestricted but approved colors are limited so as not to affect the robotic image processing systems used by all the respective teams participating in SSL competitions. Figure 1 shows the submarkers used by our researchers — who are also members of Aichi Prefectural University's RoboDragons team. A rectangular submarker (105mm$\times$ 16.5mm) was used to determine the orientation of each robot, and small circle submarkers (1$\sim$ 4 pieces, 8.5mm diameter) were used to determine the ID of each robot. Our image processing system was programmed to detect these markers.

2.2 Image Processing System

The CPU installed in the host computer is a Pentium Xeon 2GHz and the OS is Windows 2000. A progressive scanning camera (DXC-9000, SONY) avoids the problem of differences between odd and even frames caused by the high-speed movement of each robot.

A global vision camera is set at 3.0m over the soccer field. Since the length of the field's side-line, including the goal area, is about 3.2m, at least a 56 degree view angle is needed. In our system, a wide lens attachment (Fujinon, WCV-65, $\times$ 0.75) covers this range. The size of the global vision image grabbed by the frame grabber (Matrox, GEN/X/00/STD) is 640(W)$\times$480(H), and the resolution is 5 mm/pixel.

2.3 Image Processing Algorithm

The image processing system detects the location of each robot by using the team's color markers, and determines the orientation and the ID number (code) of each robot by using submarkers attached to the top of each robot. Figure 2 shows the flowchart of image processing. The outline of processing is shown below and the references listed [6–9] can be consulted for detailed descriptions.

Step1: (Input Image) Get an RGB image from the frame grabber which is captured through the progressive camera. Figure 3 shows an example of an input image. Figure 3(b) contains enlarged images surrounding and including the robots.

Fig. 1. Top surface of robot

Step2: (Calculation of Search Range) Calculate the search range based on the reliability of respective objects. Since reliability is an important parameter which characterizes the performance of image processing, the details of the calculation are explained later in this section. The white rectangles around the robots in Figure 4 were the search ranges. RGB color formatted images in the search ranges are then converted to YUV color formatted images. This greatly reduced computation time.

Step3: (Segmentation of Colored Region) In the same restricted ranges in Step2, simultaneous pattern matching was executed for 9 colors (max. 32 colors) in all YUV color formatted images by using the Carnegie Mellon University's color segmentation algorithm[10]. Since a real SSL game is not played under uniform light conditions, the intensity and color spectrum are not uniform over the soccer field. Therefore, we assigned several colors as possible colors for each object. We assigned 2 colors for the ball, 2 colors for each team color and 3 colors for the areas that we wanted to remove from processing. This method realized robust color extraction under non-uniform lighting conditions.

Step4: (Labeling) Apply the first propagation in the labeling algorithm, which we developed last year[9], to label the object region. Figure 5 shows the result. In this algorithm, the processing of interlaced images was not applied, since we used non-interlaced images.

Step5: (Selection of Objects) Detect a team's marker region and expand that region. Then, detect all ID markers and the rectangular submarker in the expanded region. The ID markers' area and the rectangular submarker's area were distinguished by their size. Figure 6 shows this result.

Step6: (Calculation of IDs and Directions) Calculate the ID and the rough orientation of each robot by the numbers and the positions of all circular submarkers, respectively. The resolution of the angle was about 8 degrees.

Step7: (Calculation of Modified Directions) Calculate the precise orientation of each robot by detecting the long edges of each rectangular submarker and apply the least mean square method to the detected edges. The precision went up to less than 1 degree.

Step8: (Record Positions and Directions) Record the current positions and directions.

Step9: (Output Object IDs, Positions and Directions) Convert the objects' positions from the camera coordinates to the world's coordinates.

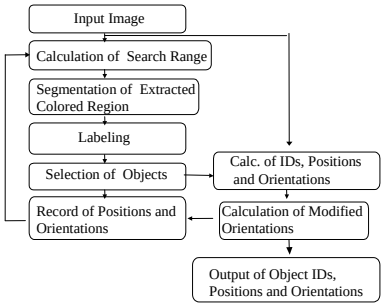

Fig. 2. Flowchart of image processing

We utilized the reliability factor to decide the search range in Step2 and Step3. Reliability indicates the degree to which the results from the image processing are correct. A wider range should be searched if the reliability is low. On the contrary, it is adequate to search in a restricted range if the reliability is high.

We defined 4 levels of reliability, i.e. non-, low-, intermediate- and high-reliability levels. The reliability level was updated every frame cycle (i.e. 60 times per second). Basically, it went up 1 level if the object detection ended in success, otherwise it went down 1 level.

A decrease in the reliability level made our search range wider and caused an increase in computation time. However, our team's information management system prevented the reliability level from excessive decreases. Such cases happen whenever a ball was occluded, since that ball detection ended in failure. Our information management system kept the reliability level at 2 (intermediate).

The search range was restricted when the reliability level was within 1–3, i.e. the range of 20 $\times$ 20 pixels, 30 $\times$ 30 pixels and 60 $\times$ 60 pixels was searched when the reliability level was 3, 2 and 1, respectively. 20 $\times$ 20 pixels range was about 10 cm $\times$ 10 cm in the real field. This search range worked for tracking a moving object up to 3m/sec.

3 Cooperative Control Algorithm

There are many types of robotic cooperative play; some examples are: pass play, defending play and assist play. In this section, the pass play algorithm is explained. The algorithms for the passing and receiving robots are given below.

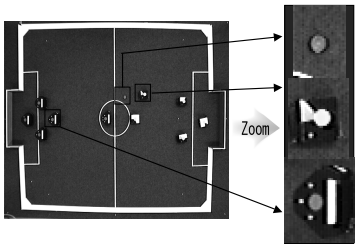

(a) global vision image (b) enlarged image

Fig. 3. An example of a grabbed image from a global vision camera

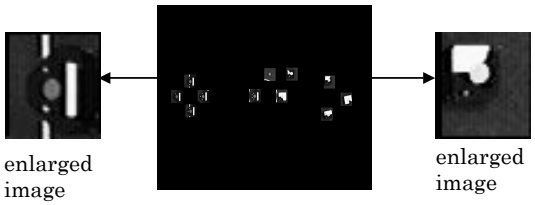

Fig. 4. Restricted region to be searched (whitened area) and enlarged images

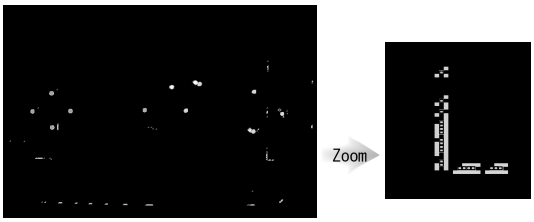

Straight lines of width 1 pixel will be recognized as separated objects. They are easily removed by area thresholding.

Fig. 5. An example of line noises to be deleted by the proposed labeling algorithm

(b) enlarged image

(a) the result of marker extraction

Fig. 6. The result of marker extraction

First, variables and flags are defined. Let the line connecting the center of the passing robot and the center of the receiving robot be $Line_A$, and let $Line_B$ be the perpendicular line extending from the center of the passing robot's face (e.g. the flat front surface of the robot). Let the angle between $Line_A$ and $Line_B$ be θ. Let the direction flag and stabilization flag be Dir and $PassCounter$, respectively.

[Initialization steps]

Step 1: Decide the rotation speed v_r based on the velocity profile shown in Figure 7. v_r depends on θ. Start rotation.

Step 2: Start dribbling device.

Step 3: If there is an obstacle on $Line_A$, then compute which side of $Line_A$ the center of that obstacle is located. If it located on the left-hand side of the passing robot, then set Dir to 1, otherwise -1. If there is no obstacle on $Line_A$, then set Dir to 0.

[Passing Action Algorithm Steps]

Step 1: Do the preceding initialization steps 1 to 3.

Step 2: If Dir is not 0, then set $PassCounter$ to 0 and go to Step 5.

Step 3: Go along $Line_B$ at a speed of v_{ps}.

Step 4: If $|\theta|$ is less than θ_{ps} and the distance between the ball and the passing robot is less than d_{min}, then increase $PassCounter$ by 1. If $PassCounter$ is greater than n_ps and $|\theta|$ is less than θ_{min}, then start the kicking device. Reset $PassCounter$.

Step 5: Wait for the next frame cycle. Go to step 1.

In the above, $v_{ps}, \theta_{ps}, d_{min}, n_{ps}, \theta_{min}$ are constants and are determined by the experiments.

[Receiving Action Algorithm Steps]

Step 1: Do the preceding initialization steps 1 to 3.

Step 2: If Dir is not 0, then go in the direction of $Dir \times \theta_{rec}$ from $Line_B$ at a speed of $\min(v_{rec}, c_{rec} \times distance\_between\_ball\_and\_Line_A)$.

Step 3: Wait for the next frame cycle. Go to Step 1.

In the above, $v_{rec}, \theta_{rec}, c_{rec}$ are constants and are determined by the experiments.

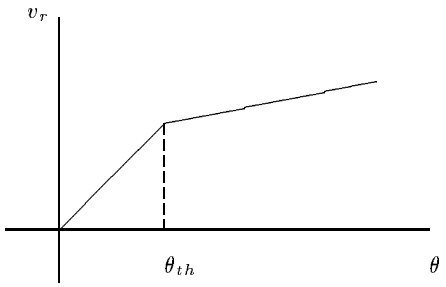

Fig. 7. Velocity profile

4 Catching Mechanism and its Analysis

4.1 Robot Mechanism

Any robot used for this type of cooperative play must be constructed so as to execute the commands given, such as moving, shooting and dribbling. Figure 8 shows our robot. Our robot has 3 omni-wheels and can move in any direction. As shown in Figure 8 (a), 3 DC motors with encoders have been used (FAULHAVER) with a gear ratio of 9.7:1. The kicking device mounted is driven by a solenoid (SINDENGEN) (Figure 8 (a) below). It can kick the ball at a maximum speed of about 3m/sec. The dribbling device utilizes a rotating roller to give backspin to the ball. The uncovered robot in Figure 8 (b) shows the dribbling roller.

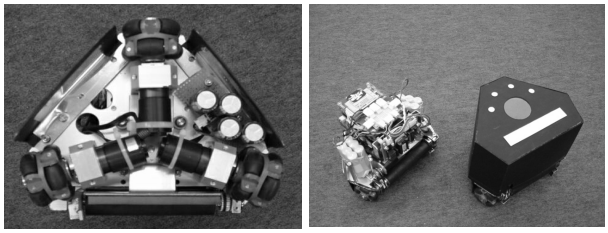

(a) omni-directional drive.

(b) appearance of our robot.

Fig. 8. Our robot system

There are two important technical issues to overcome in order torealize pass play. One is the correct recognition of the position and the orientation of each robot and the ball used. The other is the mechanism utilized to catch the ball. Regarding the former difficulty, our precise and high-speed image processing system solved the problem as described in section 2, and for the latter challenge, our system resolved the problem by adding a shock absorption mechanism to the dribbling device. It may be natural to use a spring like the Cornell University's BigRed, but our team realized it by another method.

The dribbling device is attached in front of the robot as shown in Figure 8(b). The dribbling roller, which is made of rubber, rotates, gives backspin to a given ball and can hold that ball as well. However, because the roller is hard enough not to bite into the ball which is also hard, the ball will bounce off of it if the dribbling device receives a ball travelling at a high rate of speed. To solve this problem, the team made the joint of the roller - usually attached firmly to the robot's body - looser than normal thus making it possible for it to move upward slightly so as to sufficiently absorb the impact of the ball. Still, it remains necessary to adjust the degree of looseness depending on the surface characteristics of the carpet used on a specific robotic soccer field.

4.2 Modeling of Catching Device

Since our system realizes a shock absorption mechanism by adding additional space to the jointed part of the dribbling roller, we analyzed it by three simplified physics models, (a) at the impact, (b) transition to the stable state, and (c) in the stable state.

(a) Impact model

Let the angle between the horizontal line and the line crossing to the centers of the roller and the ball be θ, and let m_R and m_B, ν_R and ν_B be mass and velocity of the roller and the ball, respectively, in the world $X-Y$ coordinates as shown in Figure 9. Let the components of ν_R and ν_B be $(\nu_{R,x}, \nu_{R,y})$ and $(\nu_{B,x}, \nu_{B,y})$ in the local $x-y$ coordinates which is parallel to the tangent line and the normal line at the collision point as shown in Figure 9.

First, by modeling the collision without rotation of the roller and the ball by the law of conservation of moment, the following equations for the y-coordinate,

$$\nu_{B,y}^{'} - \nu_{R,y}^{'} = -e_y(\nu_{B,y} - \nu_{R,y}) \tag{1}$$

$$m_B\nu_{B,y} + m_R\nu_{R,y} = m_B\nu_{B,y}^{'} + m_R\nu_{R,y}^{'} \tag{2}$$

were obtained (here a dash denotes the velocity after collision and e_y is the coefficient of rebound for y-coordinate). In the same way, for x- coordinate, the equation:

$$\nu_{B,x}^{'} - \nu_{R,x}^{'} = e_x(\nu_{B,x} - \nu_{R,x}) \tag{3}$$

$$m_B\nu_{B,x} + m_R\nu_{R,x} = m_B\nu_{B,x}^{'} + m_R\nu_{R,x}^{'} \tag{4}$$

were obtained, and the collision of the ball and roller is modeled when they are assumed as a particle.

Since the roller and the ball rotate, it is necessary to introduce some equations concerning their angular momentum. Let the moment of inertia and angular velocity be I and ω, respectively. From the law of conservation of angular momentum,

$$I_B\omega_B + I_R\omega_R = I_B\omega_B^{'} + I_R\omega_R^{'} \tag{5}$$

and the following equations,

$$r_B\omega_B = \nu_{B,x} \ , \ r_R\omega_R = \nu_{R,x} \ , \ r_B\omega_B^{'} = \nu_{B,x}^{'} \ , \ r_R\omega_R^{'} = \nu_{R,x}^{'} \tag{6}$$

were realized at the collision point (here, r_B, r_R are the radius of the ball and roller, respectively). Since our system utilized a rubber cylinder, the moments of inertia I_R and I_B were easily calculated as $I_R = \frac{1}{2}r_R^2 m_R$ and $I_B = \frac{2}{5}r_B^2 m_B$, respectively. The solutions of $\nu_{R,x}^{'}$, $\nu_{R,y}^{'}$, $\nu_{B,x}^{'}$, $\nu_{B,y}^{'}$ at the impact were calculated by solving equations (1) $\sim$ (6).

(b) Transition model

The center of gravity of the ball repeated the reflection after the impact as shown in Figure 10. It is sufficient to consider the movement of the center if the angle θ varies within the range of a few degree during the transition. Precise analysis

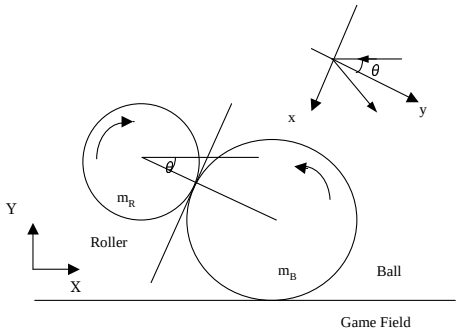

Fig. 9. Physical situation at a the impact

and modeling will be one of our future works, but it is possible to realize a simpler model as follows if the relation $e_x \equiv e_y$ was satisfied in the $x-y$ local coordinates.

Reflection angle increased reflection by reflection as shown in Figure 10, namely $\theta, 2\theta, 3\theta, ..., n\theta, ...$. After n times reflections, it exceeded $\pi/2$ and the ball returned back to the inverse direction. Figure 11 shows the case of $\theta = \pi/4$. In this case, the ball rebounded in a short time and if the roller moved in the direction illustrated by the arrows in order to absorb the shock, these angular relations were satisfied during transition.

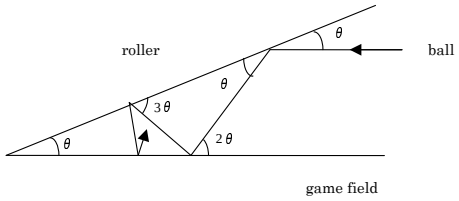

Fig. 10. Reflections of ball in the transition

(c) Stable model

Let the reactions be N_B, N_R and let the coefficients of kinetic friction be μ_1, μ_2 as shown in Figure 12. The equations of motion for the ball were as follows.

$$\text{For X} - \text{direction}: \quad -\mu_1 N_B + N_R \cos\theta - \mu_2 N_B \sin\theta = 0 \tag{7}$$

$$\text{For Y} - \text{direction}: \quad N_B - m_B g - N_R \sin\theta - \mu_2 N_R \cos\theta = 0 \tag{8}$$

By solving equations (7) and (8), the solutions for N_B, N_R were obtained as follows.

$$N_R = \frac{\mu_1 m_B g}{-(\mu_1+\mu_2)\sin\theta + (1-\mu_1\mu_2)\cos\theta} \tag{9}$$

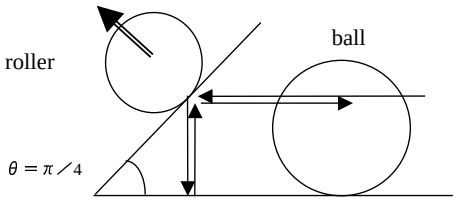

Fig. 11. An example of shock absorption at $\theta = \pi/4$

$$N_B = \frac{(\cos\theta - \mu_2 \sin\theta) m_B g}{-(\mu_1 + \mu_2)\sin\theta + (1 - \mu_1\mu_2)\cos\theta} \tag{10}$$

So the force by backspin of the ball was derived as

$$\begin{aligned} f = \mu_1 N_B &= \frac{\mu_1(\cos\theta - \mu_2 \sin\theta) m_B g}{-(\mu_1 + \mu_2)\sin\theta + (1 - \mu_1\mu_2)\cos\theta} \\ &= \frac{\mu_1(1 - \mu_2 \tan\theta) m_B g}{1 - \mu_1\mu_2 - (\mu_1 + \mu_2)\tan\theta} \end{aligned} \tag{11}$$

From equation (11), the following equations were obtained.

$$\frac{\partial f}{\partial \theta} = \frac{\mu_1^2(1 + \mu_2^2) m_B g}{\{1 - \mu_1\mu_2 - (\mu_1 + \mu_2)\tan\theta\}^2 \cos^2\theta} \tag{12}$$

$$\frac{\partial f}{\partial \mu_1} = \frac{(1 - \mu_2 \tan\theta)^2 m_B g}{\{1 - \mu_1\mu_2 - (\mu_1 + \mu_2)\tan\theta\}^2} \tag{13}$$

$$\frac{\partial f}{\partial \mu_2} = \frac{\mu_1^2(1 + \tan^2\theta) m_B g}{\{1 - \mu_1\mu_2 - (\mu_1 + \mu_2)\tan\theta\}^2} \tag{14}$$

It is easily known that the larger force f could be obtained according to the increase of θ because $\frac{\partial f}{\partial \theta} > 0$ and $f|_{\theta=0} > 0$. It is important that f has a critical point at $\theta = \arctan\frac{1}{\mu_2}$. At this point, f became 0.

5 Considerations

From the viewpoint of mechanical performance, we confirmed the effectiveness of using the dribbling and kicking devices. The dribbling devices worked well except in cases where the coefficient of kinetic friction of a SSL field's carpet surface was high and the robot lost a ball around the wall of the soccer field.

Regarding the performance of the image processing system, it was experimentally confirmed that angle accuracy is sufficient to realize cooperative play. Experimental results are shown in Table 1 with the condition that two incandescent lights were added to the existing fluorescent lights to make the environment close to an actual game environment. As a result, the luminosity value on the

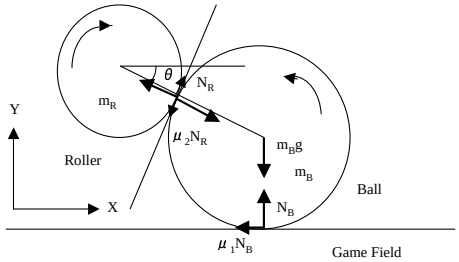

Fig. 12. Stable model by dribbling device

soccer field was set to 450-800 lux. In the ID detection experiment, five robots were placed at the free kick markers and at the center of the field, and each robot's ID was recognized 10,000 times with the condition that the robots did not move. If the distance between the recognized position of each robot and its planned position was less than 10cm, the recognition succeeded, but otherwise failed.

The accuracy of angle detection was measured on nine points on the field and the orientation of each robot was set to 0, 45, 90 and 135 degrees at each setting point. It was measured 1,000 times at each point, and the maximum angle error was calculated from the real position. There was no place on the field where ID's and submarkers could not be detected.

The recognition rates for the objects, ball, team color marker, and submarkers, were evaluated during a real game. Although the intensity of lights on the field is set at 700–1000 lux by regulation, it actually varies by the lighting condition. From actual matches, it was confirmed that our image processing system could extract all objects ith the condition that the intensity was about 200 lux.

In our image processing system, the whole image was searched only when (1) just after the game started, (2) a ball was occluded completely for some period of time, and (3) shooting speed exceeded 5m/sec. Even though it took a long time for a complete image search, it was confirmed that it worked at 20msec/frame. Our system could thus defend against a fast ball even if it was shot from the region occluded by a robot.

Table 1. Experimental results of image processing performance

Experimental item	Planned	Result
ID recognition ratio in a static mode [%]	100.00	99.68
ID recognition ratio in a dynamic mode [%]	100.00	99.61
Maximum deviation for the position [cm]	0.50	0.097
Maximum deviation for the angle [deg]	1.00	0.78
Processing time [msec]	16.7	1.33

6 Conclusions

This paper discussed the algorithms, the robot mechanism and image processing method to realize cooperative play in RoboCup SSL. Key features in our system are simple pass algorithms, implementation of dribbling and kicking devices, and high speed and robust image processing method. In particular, the visual feedback system of every 1/60 seconds realized high speed tracking of a ball moving at 3.0m/sec. From the viewpoint of image processing, if the light includes a wide spectrum like natural light does, a more robust method will be required, because color blur appears around the boundary of an object to be detected due to optical color aberration. Light with a wide dynamic range like a spotlight also bothers our image processing system; therefore, more robust algorithms for dealing with this problem will need to be developed. From the viewpoint of kicking device mechanism, further analysis and modeling of ball catching and shock absorption are expected to be conducted in the futur.

Acknowledgement

This paper was partially supported by The Hibi Research Grant, AI Research Promotion Foundation and the RoboCup Japanese Committee grant.

References

1. http://www.robocup2002.org/
2. M.Veloso, E.Pagello, and H.Kitano (Eds.), "RoboCup-99: Robot Soccer WorldCup III", Springer (June 2000)
3. P.Stone, T.Balch and G.Kraetzschmar (Eds.), "RoboCup 2000:Robot Soccer WorldCup IV", Springer (March 2000)
4. A.Brik, S.Coradeschi, and S.Tadokoro (Eds.), "RoboCup 2001:Robot Soccer WorldCup V", Springer (March 2002)
5. G.A.Kaminka, P.U.Lima and R.Rojas (Eds.), "RoboCup 2002:Robot Soccer WorldCup VI", The 2002 International RoboCup Symposium PreProceedings, Fukuoka, (June 2002)
6. Y.Kodama and K.Murakami, "Small-Size Robot Extraction Method by High-speed Image Processing for RoboCup", Proc. of VIEW2002, Yokohama, (Dec.2002) (In Japanese)
7. S.Hibino, Y.Kodama, T.Iida, K.Kato, S.Kondo, K.Murakami, and T.Naruse, "System configuration of RoboDragons team in RoboCup small- size league", Proc. of SI2002, Kobe, (Dec.2002) (In Japanese)
8. Y.Kodama, S.Hibino, K.Murakami, and T.Naruse, "Small Robot Detection by Using Image Processing and its Application to Action Planning and Action Analysis", Proc.of MIRU2002, Vol.1, pp.223-228, Nagoya, (July 2002) (In Japanese)
9. S.Hibino, Y.Kodama, Y.Nagasaka, T.Takahashi, K.Murakami, and T.Naruse, "Fast image processing and flexible path generation system for RoboCup small size league", The 2002 International RoboCup Symposium Pre-Proceedings, pp.45-57, Fukuoka, (June 2002)
10. Bruce, J., Balch, T. and Veloso, M.: "Fast and Inexpensive Color Image Segmentation for Interactive Robots", Proc. of IROS '00, pp. 2061-2066 (2000)